14. Rahn, T. & Wahlen, M. Stable isotope enrichment in stratospheric nitrous oxide. *Science* **278,** 1776–1778 (1997).
15. Dore, J. E., Popp, B. N., Karl, D. M. & Sansone, F. J. A large source of atmospheric nitrous oxide from subtropical North Pacific surface waters. *Nature* **396,** 63–66 (1998).
16. Thiemens, M. H. & Trogler, W. C. Nylon production: An unknown source of atmospheric nitrous oxide. *Science* **251,** 932–934 (1991).
17. Cliff, S. S. & Thiemens, M. H. High-precision isotopic determination of the $^{18}O/^{16}O$ and $^{17}O/^{16}O$ ratios in nitrous oxide. *Anal. Chem.* **66,** 2791–2793 (1994).
18. Cliff, S. S. & Thiemens, M. H. The $^{18}O/^{16}O$ and $^{17}O/^{16}O$ ratios in atmospheric nitrous oxide: A mass-independent anomaly. *Science* **278,** 1774–1776 (1997).
19. Cliff, S. S., Brenninkmeijer, C. A. M. & Thiemens, M. H. First measurement of the $^{18}O/^{16}O$ and $^{17}O/^{16}O$ ratios in stratospheric nitrous oxide: A mass independent anomaly. *J. Geophys. Res.* **104,** 16171–16175 (1999).
20. Rahn, T., Zhang, H., Wahlen, M. & Blake, G. A. Stable isotope fractionation during ultraviolet photolysis of N_2O. *Geophys. Res. Lett.* **25,** 4489–4492 (1998).
21. Yung Y. L. & Miller, C. E. Isotopic fractionation of stratospheric nitrous oxide. *Science* **278,** 1778–1780 (1997).
22. Johnston, J. C., Cliff, S. S. & Thiemens, M. H. Measurement of multioxygen isotopic ($\delta^{18}O$ and $\delta^{17}O$) fractionation factors in the stratospheric sink reactions of nitrous oxide. *J. Geophys. Res.* **100,** 16801–116804 (1995).
23. Holton, J. R. On the global exchange of mass between the stratosphere and troposphere. *J. Atmos. Sci.* **47,** 392–395 (1990).
24. Kroeze, C, Mosier, A. & Bouwman, L. Closing the global N_2O budget: A retrospective analysis 1500–1994. *Glob. Biogeochem. Cycles* **13,** 1–8 (1999).
25. Zipf, E. C. & Prasad, S. S. Experimental evidence that excited ozone is a source of nitrous oxide. *Geophys. Res. Lett.* **25,** 4333–4336 (1998).
26. Friedman, L. & Bigeleisen, J. Oxygen and nitrogen isotope effects in the decomposition of ammonium nitrate. *J. Chem. Phys.* **18,** 1325–1331 (1950).
27. Begun, G. M. & Landau, L. Mass spectra and metastable transitions in isotopic nitrous oxide. *J. Chem. Phys.* **35,** 547–551 (1961).
28. Richardson, W. S. & Wilson, E. B. Jr The infra-red spectrum of $^{15}N^{14}NO$ and the force constants of nitrous oxide. *J. Chem. Phys.* **18,** 694–696 (1950).
29. Toyoda, S. & Yoshida, N. Determination of nitrogen isotopomers of nitrous oxide on a modified isotope-ratio mass spectrometer. *Anal. Chem.* **71,** 4711–4718 (1999).
30. Brenninkmeijer, C. A. M. & Röckmann, T. Mass spectrometry of the intra-molecular nitrogen isotope distribution of environmental nitrous oxide using fragment-ion analysis. *Rapid Commun. Mass Spectrom.* **13,** 2028–2033 (1999).

Acknowledgements

We thank the members of the balloon launch group of The Institute of Space and Astronautical Science, and the cryogenic sampling group, for cooperation in the stratospheric sampling. We thank M. Thiemens for comments that improved an earlier version of the manuscript.

Correspondence and requests for materials should be addressed to N.Y. (e-mail: naoyoshi@depe.titech.ac.jp).

Simulated influences of Lake Agassiz on the climate of central North America 11,000 years ago

S. W. Hostetler*, P. J. Bartlein†, P. U. Clark‡, E. E. Small§ & A. M. Solomon‖

* *US Geological Survey, Corvallis, Oregon 97333, USA*
† *Department of Geography, University of Oregon, Eugene, Oregon 97403, USA*
‡ *Department of Geosciences, Oregon State University, Corvallis, Oregon 97333, USA*
§ *Department of Earth Sciences, New Mexico Tech, Soccoro, New Mexico 87801, USA*
‖ *US Environmental Protection Agency, Corvallis, Oregon 97333, USA*

Eleven thousand years ago, large lakes existed in central and eastern North America along the margin of the Laurentide Ice Sheet. The large-scale North American climate at this time has been simulated with atmospheric general circulation models[1,2], but these relatively coarse global models do not resolve potentially important features of the mesoscale circulation that arise from interactions among the atmosphere, ice sheet, and proglacial lakes. Here we present simulations of the climate of central and eastern North America 11,000 years ago with a high-resolution, regional climate model nested within a general circulation model. The simulated climate is in general agreement with that inferred from palaeoecological evidence. Our experiments indicate that through mesoscale atmospheric feedbacks, the annual delivery of moisture to the Laurentide Ice Sheet was diminished at times of a large, cold Lake Agassiz relative to periods of lower lake stands. The resulting changes in the mass balance of the ice sheet may have contributed to fluctuations of the ice margin, thus affecting the routing of fresh water to the North Atlantic Ocean. A retreating ice margin during periods of high lake level may have opened an outlet for discharge of Lake Agassiz into the North Atlantic. A subsequent advance of the ice margin due to greater moisture delivery associated with a low lake level could have dammed the outlet, thereby reducing discharge to the North Atlantic. These variations may have been decisive in causing the Younger Dryas cold event[3,4].

We used the GENESIS v2.01 atmosphere general circulation model (AGCM) to simulate the global climate of 11 kyr BP (11,000 years before present). The simulations were run at a nominal atmospheric resolution of 3.75° by 3.75° (latitude by longitude) with 18 vertical layers and an interactive, land–surface physics package[1,5]. Specified boundary conditions for the AGCM included 11-kyr BP values for eccentricity, obliquity and precession; an atmospheric CO_2 concentration of 270 parts per million by volume, p.p.m.v.; Dorman-Sellers global vegetation[6]; and reconstructions of continental ice sheets 11 kyr ago[7,8]. Global sea surface temperatures (SSTs) and sea ice were computed by GENESIS using a 50-m mixed-layer ocean model. The GENESIS simulation was initialized from an existing 11-kyr BP simulation and run continuously for 20 years to ensure that the simulated climate and SSTs were in equilibrium. The last five years of the GENESIS simulations were used to derive initial and continuous 12-hour (diurnal) lateral boundary conditions (vertical profiles of temperature, humidity, wind and pressure) for the regional model.

The global climate simulation is similar to others for the period around 11 kyr BP (refs 1, 2) which typically display the interplay of the waning continental ice sheets and rising insolation on Northern Hemisphere atmospheric circulation (Fig. 1). Over the continental interior of North America, the features of the simulated 11-kyr BP climate include: greater summer warming in regions farther from the ice sheet (which occurs in response to the interaction between the large expanse of ice sheet and greater-than-present summer insolation), colder-than-present winter temperatures (which occurs in response to the negative winter insolation anomaly), and precipitation patterns that reflect the reorganization of atmospheric circulation by the ice sheet and insolation. In the AGCM, however, finer-scale topographic detail and surface–atmosphere feedbacks that may be important to climate at regional scales are not resolved.

To resolve these regional-scale feedbacks and processes, we applied the NCAR RegCM2 regional climate model. Our palaeoclimate version of the RegCM2 has an interactive land-surface physics package (the biosphere-atmosphere transfer scheme, BATS) and includes an interactive, one-dimensional (vertical) lake model[9–13]. A domain size of 3,375 km × 3,825 km, a horizontal grid spacing of 45 km × 45 km (yielding ~80 RegCM2 grid points for each GENESIS grid box) and 17 vertical levels, extending from ~40 m above the ground to the upper troposphere, were used in the model. A total of 249 lake grid points were prescribed: 185 represent Lake Agassiz (ranging in depth from 10 to 200 m, ref. 14), and the remainder represent other large lakes (all depths set to 25 m). As in the GENESIS simulation, we specified orbital parameters and CO_2 concentration at 11 kyr BP, and a higher-resolution version of the reconstructed Laurentide Ice Sheet (LIS)[7] was used in the RegCM2.

We constrained the simulated temperatures of the grid points representing Lake Agassiz to be ≤5 °C based on several lines of evidence. During the time of our simulation, the ostracod *Candona*

subtriangulata, which records sub-surface temperatures and requires cold (~5 °C) water conditions, overwhelmingly dominated the ostracod assemblage of the Lake Agassiz basin[15]. The lake was probably unstratified (polymictic) at 11 kyr BP (ref. 16), so the water column of the open lake probably remained at or below 5 °C during ice-free periods. Additional support for cold water temperatures comes from evidence of extensive sediment scraping by lake ice or icebergs[17], estimated meltwater inputs from the LIS of at least 0.02 Sv (ref. 18) and protrusion of the LIS into the lake water along ~1,700 km of the eastern shoreline which may have formed an ice shelf. Partitioning of the excess heat associated with the constrained temperatures is discussed below. The temperatures of the other large lakes were not constrained.

To quantify the influence of Lake Agassiz on the regional climate, two simulations using RegCM were completed: (1) a continuous 4.5-year-long simulation in which the 11–kyr palaeogeography (that is, LIS, vegetation, proglacial lakes) was specified[2,19] and (2) a parallel 4.5-year-long simulation in which all lake grid points replaced by the 11-kyr reconstructed vegetation distributions interpolated from the adjacent non-lake grid points. (The first half-year of each simulations is excluded from our analyses to allow for initialization of the model.) We do not include a control simulation for three reasons. First, the model reproduces the present climate of the region adequately[20,21]. Second, any model bias evident in simulation of the present climate would be small compared with the differences between the 11-kyr simulation and the observed climate data (for example, presence versus absence of the LIS). Third, we compare the simulated climate with that inferred from fossil-pollen data.

The simulated patterns of temperatures and anomalies in both January and July compare well with those inferred for 11 kyr BP from fossil-pollen data (Fig. 2) and reflect the dominant effect of the LIS on the climate of central and eastern North America. Summer temperature gradients as high as 3.3 °C per 100 km are located ~450 km south of the margin of the LIS, while gradients as high as 5.5 °C per 100 km occur closer to the ice sheet, gradients much higher than the present gradient of ~1 °C per 100 km (ref. 22) and that simulated by the AGCM. A gradient of 3.3 °C per 100 km is consistent with the pollen data[2,23]. The gradient of 5.5 °C per 100 km is consistent with reconstructions inferred from fossil-midge data from eastern North America[24], but is steeper than that inferred from pollen data, which may reflect the absence of enough pollen sites along the ice sheet to resolve the steeper gradient.

Over central and eastern North America, the magnitude of the moisture anomalies and the location of their gradients are in generally good agreement with palaeodata[2,25] (Fig. 2), although in detail, some differences exist between the data and model results. For example, at 11 kyr BP, simulated precipitation is reduced, relative to present, south of Lake Agassiz over central Minnesota; this is consistent with the inference of cooler and drier conditions from pollen data at Elk Lake[26], but inconsistent with inferences of wetter conditions inferred from isotopic data at nearby Deep Lake[27], attributed to lake-induced precipitation. Additionally, the suggestion of wetter- and warmer-than-present conditions along the southwestern shore of Lake Agassiz may not be comparable to model results because the pollen data from that area present a known 'no-analog' assemblage[28]. Although our results are in general agreement with palaeodata from central and eastern North America, complete reconciliation of the record of large temporal and spatial transitions in climate that occurred around 11 kyr BP will require detailed compilation of data chronologies and comparison of multiple climate proxies.

Anticyclonic winds at the surface originate from high-pressure centres located over high elevations of the ice sheet (Fig. 3). The flow of the winds is directed downward by the topography of the ice and laterally along the margin by thermal gradients set up between the ice and Lake Agassiz. The simulated anticyclonic winds penetrate a limited distance into adjacent ice-free areas, indicating that anticyclonic flow, as simulated by the RegCM, probably would not have played a significant role in forming regional aeolian features at 11 kyr BP.

From the anomalies between the simulation that included the lakes and the simulation in which the lakes were replaced by vegetation ('lake' minus 'no-lake'), we see that the primary atmospheric effect of Lake Agassiz is the thermal forcing associated with the seasonal cycle of heat storage. This induces changes in atmospheric pressure, circulation (Fig. 3) and moisture (not shown). Circulation changes are evident, for example, in July when, relative to the no-lake simulation, the cold surface of Lake Agassiz modifies atmospheric pressure cells, leading to stronger anticyclonic flow at the surface and a tendency for more cyclonic flow in the mid-troposphere. (Fig. 3). This flow blocks penetration of winds and moisture from the south and west. A related effect of this circulation pattern is a reduction in atmospheric moisture over the lake and the adjacent ice margin; this results from less evaporation from the cold lake surface than evapotranspiration from the warmer vegetation.

The circulation patterns associated with the lake cause a coherent pattern of substantially reduced precipitation that extends eastward along the ice margin, across the Superior Lobe of the ice sheet that dammed eastern outlets of Lake Agassiz and northeastward into the

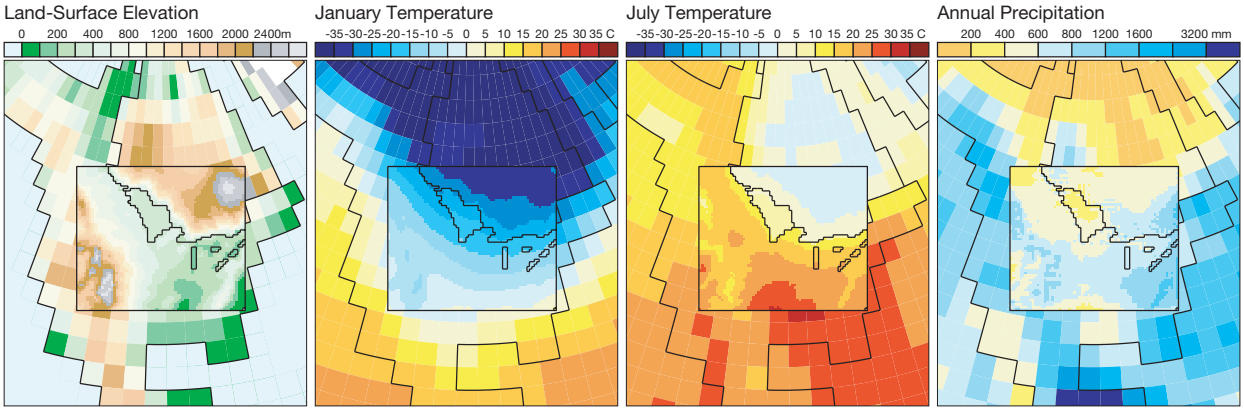

Figure 1 Surface elevation and simulated climate fields over North America at 11 kyr BP. The nominal resolution of the GENESIS atmosphere model, shown as the coarse continental outline and large grid boxes, is 3.75° by 3.75° (400 km by 400 km) latitude by longitude. The resolution of the RegCM2 model used in this study (inset box) is 45 km by 45 km, which yields ~80 grid cells for each AGCM grid cell. The AGCM-derived boundary conditions are assimilated into the RegCM2 every 12 h over an additional 8 grid-point strip, roughly the distance of one AGCM grid cell, along the entire boundary of the model. The figure illustrates that the patterns simulated by the RegCM2 are not simple interpolations of the patterns in the AGCM, but instead reflect the variations of topography and surface characteristics on the higher-resolution grid of the model.

interior of the ice sheet (Fig. 3). Annual precipitation (Fig. 2) is reduced by >120 mm (~30%) over portions of the ice sheet and the Superior Lobe, whereas July precipitation (not shown) is reduced by >50 mm (~90%) around the lake and by 40 mm (~50%) over the ice margin and into the interior. [We note that precipitation is enhanced somewhat by atmospheric heating and elevated moisture levels before the lake freezes in late autumn (November in Fig. 3) but this is offset by drying during the rest of the year.] This generally negative precipitation feedback opposes previous hypotheses[27,29], and contrasts with simulations of the US Great Basin in which lake–atmosphere feedbacks enhanced precipitation during the Last Glacial Maximum[13].

Heat in excess of that required to maintain the lake at a temperature of 5 °C (derived mainly from solar heating at the lake surface) would probably have been consumed in warming cold melt water from the LIS and in melting icebergs and shelf ice. The heat required to raise the estimated inflow of 0.02 Sv of melt water (ref. 18) from 0 °C to 5 °C is ~10^{13} MJ. Accounting for heat needed to warm the melt water, at an ice temperature of –5 °C enough excess heat is available from the constrained temperatures (~10^{14} MJ) to melt ~2,500 km^3 of ice annually, suggesting that the internal heating of the lake would have contributed to significant ablation of the ice in contact with the lake.

Our results suggest a mechanism for linking the atmosphere–lake–ice system to the retreat and advance of the Superior Lobe, which, in turn, played an important role during the last deglaciation in damming eastward-draining outlets of Lake Agassiz, and thus in controlling the routing of a substantial fraction of continental runoff to the North Atlantic[3,4,18]. During the large (Lockhart) phase of Lake Agassiz, (which pre-dates eastward drainage to the St Lawrence before 13 kyr BP), the lake would have suppressed precipitation and contributed to retreat of the ice margin in contact with lake water, reinforcing deglaciation. At ~13 kyr BP, the Superior Lobe had receded far enough to allow the lake to drain eastward to the St Lawrence River, supplying ~0.05 Sv of additional fresh water to the North Atlantic[18] which triggered the Younger Dryas cold interval[3,4]. With the lake diminished in size, moisture delivery to the ice sheet would have increased, supporting the hypothesis that the Marquette ice advance into the Superior basin was related to changes in mass balance rather than to surging or ice streaming[30]. The resulting damming of the eastern outlets would have ended the Younger Dryas cold reversal[3,4] and allowed the lake to expand to its maximum size (Emerson phase) simulated here.

Our results depend on using the geological record as guidance in limiting the maximum surface temperature of Lake Agassiz, and on the driving boundary conditions derived from GENESIS. In climate simulations, as in nature, the climate of a 5-year period may vary from that of other 5-year periods. The climate forcing arising with the interplay of the LIS and insolation is robust in controlling both the simulated large-scale (AGCM) and regional-scale (RegCM2) circulations. Taken together with the strong thermal forcing of the lake in RegCM2, our results would probably be reproducible for any different period of our GENESIS simulation, even if the actual temperature of the lake was several degrees warmer than suggested

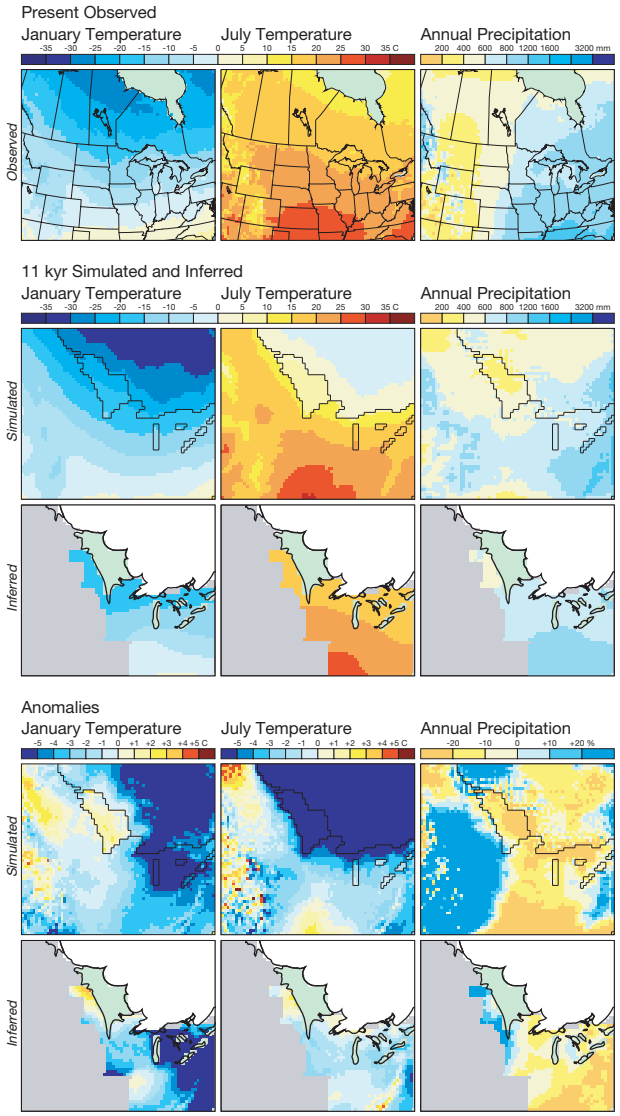

Figure 2 Simulated and inferred temperature and precipitation climatologies for 11 kyr BP. These were inferred from pollen reconstructions and simulated by the RegCM2. The anomalies are the differences between inferred or simulated data relative to observed data. Observed values are 30-year averages from instrumental records interpolated onto the model grid. Simulated values are averages over four simulated years. Inferred values are pollen-based estimates derived by averaging reconstructions for 12,000 ^{14}C yr BP (~14 kyr) and 9,000 ^{14}C yr BP (~10 kyr) (ref. 24) and interpolating the averages onto the model grid.

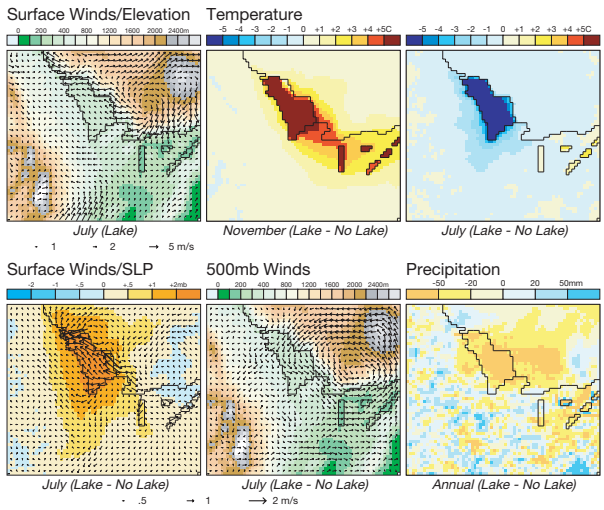

Figure 3 Selected fields for the lake simulation, and anomalies between the lake and no-lake simulations. The values are averages over four simulated years. July surface (2-m) wind vectors and upper-level (500 mb) wind anomalies are plotted over the model topography. Temperature anomalies are for the 2-m air temperature. November is the month in which maximum warming of the atmosphere by the lake occurs. July surface-wind anomalies are plotted over sea-level pressure anomalies (SLP).

by the ostracod data. The ability to simulate finer-scale climate processes in complex palaeoenvironmental settings offers the opportunity to test climate hypotheses at the landscape scale; it also suggests that a nested modelling approach will be useful in investigating a wide range of surface–atmosphere feedbacks associated with regional climates of the past, present and future. □

Received 23 July 1999; accepted 27 March 2000.

1 Pollard, D. *et al.* Climate simulations for 10000 and 6000 years BP using the GENESIS global climate model. *Paleoclimates* **2,** 183–218 (1998).
2. Bartlein, P. J. *et al.* Paleoclimate simulations for North America over the past 21,000 years: Features of the simulated climate and comparisons with paleoenvironmental data. *Quat. Sci. Rev.* **17,** 549–585 (1998).
3. Broecker, W. S. *et al.* Routing of meltwater from the Laurentide ice sheet during the Younger Dryas cold episode. *Nature* **341,** 318–321 (1989).
4. Teller, J. T. Meltwater and precipitation runoff to the North Atlantic, Arctic, and Gulf of Mexico from the Laurentide ice sheet and adjacent regions during the Younger Dryas. *Paleoceanography* **5,** 897–905 (1990).
5. Thompson, S. L. & Pollard, D. A global climate model (GENESIS) with a land-surface-transfer scheme (LSX), 1, Present-day climate. *J. Clim.* **8,** 732–761 (1995).
6. Dorman, J. L. & Sellers, P. J. A global climatology of albedo, roughness length, and stomatal resistance for atmospheric general circulation models as represented by the simple biosphere model (SiB). *J. Appl. Meteorol.* **28,** 833–855 (1989).
7. Licciardi, J. M., Clark, P. U., Jenson, J. W. & MacAyeal, D. R. Deglaciation of a soft-bedded Laurentide ice sheet. *Quat. Sci. Rev.* **17,** 427–448 (1998).
8. Peltier, W. R. Ice age paleotopography. *Science* **265,** 195–201 (1994).
9. Giorgi, F., Marinucci, M. R. & Bates, G. T. Development of a second-generation regional climate model (RegCM2), I, Boundary layer and radiative processes. *Mon. Weath. Rev.* **121,** 2794–2813 (1993).
10. Giorgi, F., Marinucci, M. R. & Bates, G. T. Development of a second-generation regional climate model (RegCM2), II, Convective processes and assimilation of boundary conditions. *Mon. Weath. Rev.* **121,** 2814–2832 (1993).
11. Hostetler, S. W. & Bartlein, P. J. in *Mechanism of Global Climate Change at Millennial Time Scales* (eds Clark, P. U., Webb, R. S. & Keigwin, L.) 313–328 (AGU Monograph Series, American Geophysical Union, Washington, DC, 1999).
12. Small, E. E., Sloan, L. C., Hostetler, S. W. & Giorgi, F. Simulating the water balance of the Aral Sea with a coupled regional climate-lake model. *J. Geophys. Res.* **104,** 6583–6602 (1999).
13. Hostetler, S. W., Giorgi, F., Bates, G. T. & Bartlein, P. J. Lake-atmosphere feedbacks associated with paleolakes Bonneville and Lahontan. *Science* **263,** 665–668 (1994).
14. Mann, J. D., Leverington, J. D., Rayburn, J. & Teller, J. T. The volume and paleobathymetry of glacial Lake Agassiz. *J. Paleolimnol.* **22,** 71–89 (1999).
15. Curry, B. B. Paleochemistry of Lakes Agassiz and Manitoba based on ostracodes. *Can. J. Earth Sci.* **34,** 699–708 (1997).
16. Mann, J. D. *et al.* Calculating the volume and heat budget of glacial Lake Agassiz. *GSA Ann. Meeting Abstr.* **29,** A111 (1997).
17. Clayton, L., Moran, S. R. & Bluemle, J. P. Intersecting minor lineations on Lake Agassiz plain. *J. Geol.* **73,** 652–656 (1965).
18. Licciardi, J. M., Teller, J. T. & Clark, P. U. in *Mechanism of Global Climate Change at Millennial Time Scales* (eds Clark, P. U., Webb, R.S. & Keigwin, L.) 177–202 (AGU Monograph Series, American Geophysical Union, Washington, DC, 1999).
19. Dyke, S. & Prest, V. K. *Map 1703A* (Geological Survey of Canada, Ottawa, 1987).
20. Bates, G. T., Hostetler, S. W. & Giorgi, F. Two-year simulation of the Great Lakes region with a coupled modeling system. *Mon. Weath. Rev.* **123,** 1505–1522 (1995).
21. Giorgi, F. *et al.* Regional nested model simulations of present day and $2XCO_2$ climate over the Great Plains of the US. *Clim. Change* **40,** 457–493 (1998).
22. Hostetler, S. W. Climate near to the edge of an ice sheet. *Nature* **385,** 393–394 (1997).
23. Webb, T., Bartlein, P. J., Harrison, S. P. & Anderson, K. H. in *Global Climates Since the Last Glacial Maximum* (eds Wright, H. E., Kutzbach, J. E., Webb, T., Ruddiman, W. F., Street-Perrott, F. A. & Bartlein, P. J.) 415–467 (Univ. Minnesota Press, 1993).
24. Levesque, A. J., Cwynar, L. C. & Walker, I. R. Exceptionally steep north-south gradients in lake temperature during the last deglaciation. *Nature* **385,** 423–426 (1997).
25. Laird, K. R., Fritz, S. C., Grimm, E. C. & Mueller, P. G. Century-scale paleoclimatic reconstruction from Moon Lake, a closed-basin lake in the northern Great Plains. *Limnol. Oceanogr.* **41,** 890–902 (1996).
26. Bartlein, P. J. & Whitlock, C. in *Elk Lake, Minnesota: Evidence for Rapid Climate Change in the North-Central United States* (eds Bradbury, J. P. & Dean, W. E.) 275–293 (Geologic Society of America, Boulder, 1993).
27. Hu, F. S., Wright, H. E., Ito, E. & Lease, K. Climate effects of glacial Lake Agassiz in the midwestern United States during the last deglaciation. *Geology* **25,** 207–210 (1997).
28. Overpeck, J. T., Webb, R. S. & Webb, T. W. Mapping eastern North American vegetation change of the past 18 ka: no-analogs and the future. *Geology* **20,** 1071–1074 (1992).
29. Teller, J. T. in *North America and Adjacent Oceans During the Last Deglaciation* (eds Ruddiman, W. F. & Wright, H. E.) 39–69 (Geological Society of America, Boulder, 1986).
30. Lowell, T. V., Larson, G. H., Hughes, J. D. & Denton, G. H. Age verification of the Lake Gribben forest bed and the Younger Dryas advance of the Laurentide Ice Sheet. *Can. J. Earth Sci.* **36,** 383–393 (1999).

Acknowledgements

We thank F. S. Hu, E. Ito, and H. E. Wright for discussions, D. Pollard and J. Teller for discussions and critical reviews, and R. Gallimore, F. Giorgi and D. Zahnle for assistance. Model simulations were conducted at NCAR and the National Environmental Super Computer (NESC) facility of the US Environmental Protection Agency. Special thanks to NESC for help in completing our model simulations. This work was supported by the US Geological Survey (S.W.H.), the National Science Foundation (P.J.B., P.U.C., E.E.S.), and the US Environmental Protection Agency (A.M.S.).

Correspondence and requests for materials should be addressed to S.W.H. (e-mail: steve@ucar.edu).

Mesozoic plate-motion history below the northeast Pacific Ocean from seismic images of the subducted Farallon slab

Hans-Peter Bunge* & Stephen P. Grand†

* *Department of Geosciences, Princeton University, Princeton, New Jersey 08544, USA*

† *Department of Geological Sciences, University of Texas, Austin, Texas 78712, USA*

The high-resolution seismic imaging of subducted oceanic slabs[1,2] has become a powerful tool for reconstructing palaeogeography[3]. The images can now be interpreted quantitatively by comparison with models of the general circulation of the Earth's mantle[4]. Here we use a three-dimensional spherical computer model of mantle convection[5,6] to show that seismic images of the subducted Farallon plate provide strong evidence for a Mesozoic period of low-angle subduction under North America. Such a period of low-angle subduction has been invoked independently to explain Rocky Mountain uplift far inland from the plate boundary during the Laramide orogeny[7]. The computer simulations also allow us to locate the largely unknown Kula–Farallon spreading plate boundary, the location of which is important for inferring the trajectories of 'suspect' terrain across the Pacific basin[8].

The geology of western North America was shaped by interaction with three major ocean plates; the Kula, Farallon and Pacific plates[9]. Their motion in the Cenozoic era has been inferred through careful reconstructions of relative plate movement[10,11]. However, reconstructing Kula and Farallon plate motion further back in time is difficult because the Pacific plate from the Mesozoic era has been almost entirely lost to subduction. The lack of old oceanic lithosphere has prompted attempts to use high-resolution tomographic models to constrain past plate motion[3]. For example, fast seismic velocity anomalies in the upper mantle shear-wave structure under North America have been related explicitly to Cenozoic subduction of the Farallon plate about 30 Myr ago[12].

Earlier Mesozoic motion (about 80 Myr ago) of the Kula and Farallon plates is now recorded in the lower mantle. In Fig. 1a we show the seismic velocity structure under North America at four depths. The images are from a recent high-resolution tomographic S-wave model[1] and are remarkably similar to an independent study based on P waves[2]. A band of high seismic velocities underlies eastern North America and marks the ancient Kula and Farallon plates.

The 1,300 km snapshot reveals two distinct trends for the slab beneath the Great Lakes region. It strikes southeast under the Canadian shield, but turns sharply south beneath the east coast of the United States. The seismic bight is strongest at 1,500-km depth, where it takes the form of a big 'hook' similar to a feature imaged recently in the deep mantle beneath the Siberian craton[3]. Under South America the tomographic model reveals a slab at 900-km and 1,100-km depth, but not below.

Geodynamic heterogeneity structure under North America